JOURNAL OF GEOPHYSICAL RESEARCH, VOL. 99, NO. B1, PAGES 729–742, JANUARY 10, 1994

Relationship between subduction and seismicity in the Mexican part of the Middle America trench

Vladimir Kostoglodov[1] and Lautaro Ponce

Instituto de Geofísica, Universidad Nacional Autónoma de México, México

Two catalogs of earthquakes in the Mexican part of the Middle America trench are analyzed to elucidate principal relations between structure of the subducting Cocos plate and seismicity. A catalog of historical events that have occurred during the last two centuries with large magnitudes ($M_s > 6.0$) is used to obtain cumulative seismic moment (M_o) and seismic moment release rate ($\dot{M}_o$) distributions along the Mexican subduction zone. The catalog of instrumentally observed earthquakes from 1963 to 1990 (International Seismological Center and U.S. Geological Survey) with $4.5 \leq m_b < 6.0$ is applied to investigate background seismicity for the region. The strength of coupling between the Cocos and North American plates would be expected to grow gradually from the southeast to the northwest according to the variation of convergence rate (V) and age (A) of the Cocos plate. This correlates in general with a steady reduction in background seismicity and a slight average increase of $\dot{M}_o$ and seismic energy release rate ($\dot{W}$). At the sites where the main fracture zones of the Cocos plate; Tehuantepec, O'Gorman, Orozco and Rivera, undergo the subduction the general correlation breaks down. The background seismicity increases at fracture zones while M_o and $\dot{M}_o$ decrease significantly. This feature is interpreted as a drop of the coupling at the areas where transform faults are being subducted. Seismic slip rates along the trench obtained from $\dot{M}_o$ are lower then the values of plate convergence rates but the average seismic slip is in agreement with the estimates from the V model (interaction between lithospheric plates at convergent zones through the viscous layer of subducted sediments). Variability of $\dot{M}_o$ and seismic slip rate in relation with tectonics should be taken into account when the seismic gap model is being used for the prediction of strong earthquakes. An examination of space-time plots for the historical catalogs supposes a probable tendency of northwest migration of strong events with a rate of $\approx$ 10 km/yr.

INTRODUCTION

The tectonics and seismicity in the western part of central Mexico are determined predominantly by the subduction of the Cocos (COCOS) and the Rivera (RIV) oceanic plates beneath the North American plate (NOAM) and by the degree of interaction (coupling) between these plates along the Middle America trench (MAT) [*Molnar and Sykes,* 1969; *Burbach et al.,* 1984; *Singh and Mortera,* 1991; *Dewey and Suárez,* 1991]. A knowledge of the relation between the subduction process and seismicity is of great importance for the prediction of disastrous earthquakes in this region. According to the hypothesis of *Ruff and Kanamori* [1980], [also *Lay et al.*, 1982; *Ruff and Kanamori,* 1983] the plate coupling in the interface zone should rise as the value of convergence rate (V) increases and reduce with the age (A) of the subducting lithosphere. A number of previous studies of seismicity in the region [e.g., *McNally and Minster,* 1981; *Burbach et al.,* 1984; *Anderson et al.,* 1989; *Singh and Mortera,* 1991] showed a general tendency of lower levels of seismicity (total number of events) and increasing cumulative seismic moment from the southeast to the northwest along the Middle America trench. This may be explained by stronger coupling of the interface in the northwest direction associated with the changes of A and V [*Singh and Mortera,* 1991]. However, an analysis of source parameters of a considerable number of large Mexican subduction zone earthquakes [e.g., *Chael and Stewart,* 1982; *Burbach et al.,* 1984; *LeFevre and McNally,* 1985; Singh and Mortera, 1991] revealed a pronounced segmentation of the seismicity pattern, with adjacent segments being bounded by the subduction of major bathymetric features such as aseismic ridges and fracture zones. *McNally and Minster* [1981] discovered a nonuniformity of seismic slip along the MAT which is caused by the subduction of Orozco fracture zone (OFZ) and Tehuantepec ridge (TR). *Anderson et al.* [1989] obtained a significant deficiency of seismic slip in the Oaxaca region, while in the other regions the slip roughly conformed to the plate motion. *Singh and Mortera* [1991] presented data illustrating sharp changes in the rupture mode of large thrust earthquakes near 99°W where the O'Gorman fracture zone (OGFZ) intersects the trench. All these observations have important bearing on the understanding of the relation between tectonics and seismicity and permit qualitative interpretation in the sense of the degree of plate coupling.

Here we let the strength of mechanical coupling at the interface zone be defined in the framework of the V model (see Appendix) as the maximum shear stress (τ_m) at the base of the overthrusting plate [*Kostoglodov,* 1988], $\tau_m \propto V/A$. In this case the relation between subduction parameters and seismicity can be expressed in a more quantitative way.

Recently, *Anderson et al.* [1989] comprehensively revised a catalog of large earthquakes in Mexico. On the basis of instrumental recordings from Uppsala, Sweden, they proposed a new relation between moment and magnitude for large thrust events in the region. We employ this catalog to conduct a detailed study of the distribution of seismic moment and seismic slip rate along the Mexican trench. The catalog of instrumentally observed earthquakes (International Seismological Center (ISC) and U.S. Geological Survey (USGS))

[1]Also at Institute of Physics of the Earth, Russian Academy of Sciences, Moscow.

Paper number 93JB01556.
0148-0227/94/93JB-01556$05.00

from 1963 to 1990 may be used simultaneously to examine background seismicity. In this study, we undertake a careful analysis of seismicity using these two catalogs in order to understand its general dependence on subduction parameters as well as to investigate the characteristic seismotectonic features of subduction of the fracture zones.

CONVERGENT TECTONICS OF CENTRAL MEXICO

The convergence rate, the age and the morphological structure of the underthrusting oceanic plate dominate the subduction tectonics and seismicity. The tectonic history of the region from 25 Ma B.P. to the Present was associated with several episodes of spreading reorganizations [*Mammerickx and Klitgord,* 1982] which probably resulted in the formation of the present spreading and subduction system by approximately 3.5 Ma (Figure 1). In the following discussion we use topographic structures from *Dirección General de Oceanografía Naval* [1987].

The Rivera microplate, if it is kinematically distinct from the COCOS, converges under the NOAM plate with a very low velocity of 0.6 - 2.0 cm/yr [*DeMets and Stein,* 1990]. Its morphological structure is puzzling. Because of a number of offsets across small transform faults, the age of this plate at the MAT varies, with values of the order of 9 Ma [*Klitgord and Mammerickx,* 1982]. The southern boundary of the RIV plate, formed as a rather wide and complex Rivera fracture zone (RFZ), intersects the MAT near 105°W (Figure 1).

Farther to the south the Cocos plate converges with the NOAM with velocity that increases moderately from 5.0 cm/yr at 104°W to 7.5 cm/yr at 94°W [*DeMets et al.,* 1990]. The main segments of the COCOS plate along the MAT are bounded by the Rivera (RFZ), Orozco (OFZ), O'Gorman (OGFZ) and Tehuantepec (TFZ) fracture zones. The age of the COCOS plate varies gradually along the MAT increasing from the northwest (7 Ma) to the southeast (23 Ma) [*Klitgord and Mammerickx,* 1982] (Figure 2).

The Orozco fracture zone with the age offset of 2 m.y. is a broad and complex topographic structure. It crosses the MAT near 102°W where the maximum depth of the trench reduces from about 5 km to 4.2 km. The segment of the COCOS between the RFZ and the OFZ has a rugged topography related to a complicated tectonic history.

The O'Gorman fracture zone is a subtle structure imposed on the otherwise smooth topography of adjacent segments of the COCOS plate. According to the model of *Klitgord and Mammerickx* [1982], this zone does not have an age offset, although *Singh and Mortera* [1991] supposed some jump of age across the OGFZ to explain the difference in rupture modes on either side of it. The OGFZ intersects the MAT at 98.8°W and decreases the maximum depth of the trench to 4.6 km.

The Tehuantepec ridge (TR) is a relatively narrow feature with an elevation more than 1 km. It can be interpreted as the northern heightened part of a broader fracture zone [*Mammerickx and Klitgord,* 1982] which cut the MAT at 95.3°W. The difference in age across the TFZ at the MAT is about 10-25 m.y. [*Couch and Woodcock,* 1981].

There is another weak linear topographic structure on the COCOS segment between the OGFZ and the TR which intersects the MAT at 97.3°W and may be recognized as a fracture zone following the model of *Klitgord and Mammerickx* [1982]. The age offset is not well known here. The maximum depth at the MAT decreases from 5.4 to 5.2 km up to 4.8 km.

The COCOS's convergence velocity vector contains a small east-southeast oblique component. Together with an oblique orientation of the main bathymetric features relative to the trench and shoreline

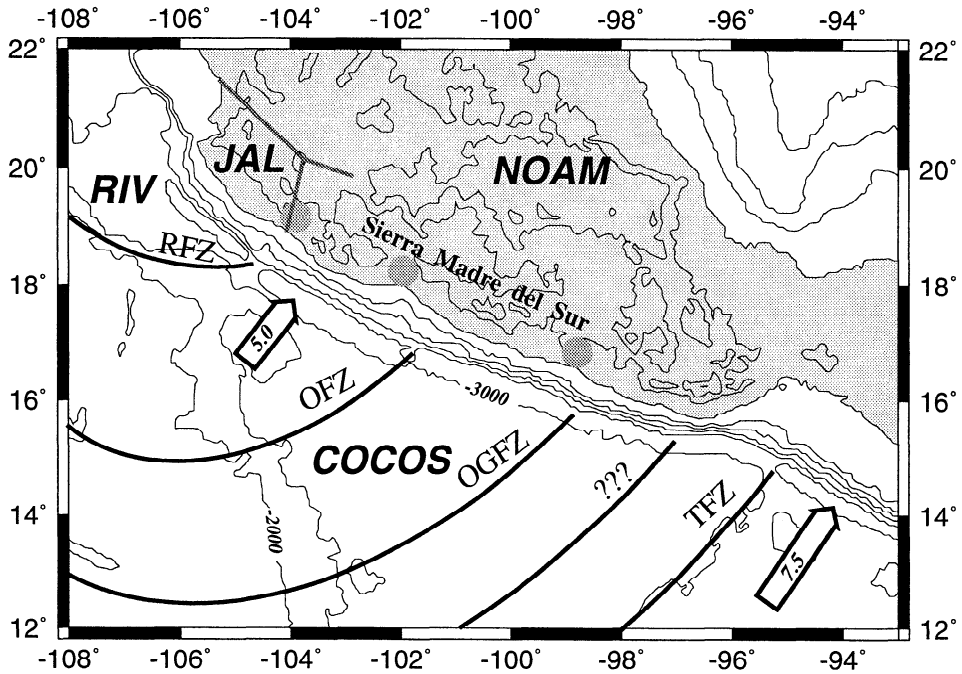

Fig. 1. Tectonic framework of the Mexican subduction zone. Long solid arcs indicate fracture zones. The Middle America Trench is contoured by the isobath of -3000 m, and the East Pacific Rise is comprised by the -2000 m isobath. Grey lines (inshore) indicate the system of Colima, Tepic-Chapala and Chapala rifts. The light grey circles (inshore) denote the locations of main river valleys. Open arrows are subduction velocity vectors with the values of velocity in centimeters per year. Abbreviations are NOAM, North American plate; COCOS, Cocos plate; RIV, Rivera plate; JAL, hypothetic Jalisco block; fracture zones: RFZ, Rivera; OFZ, Orozco; OGFZ, O'Gorman; ???, surmised fracture zone; TFZ, Tehuantepec.

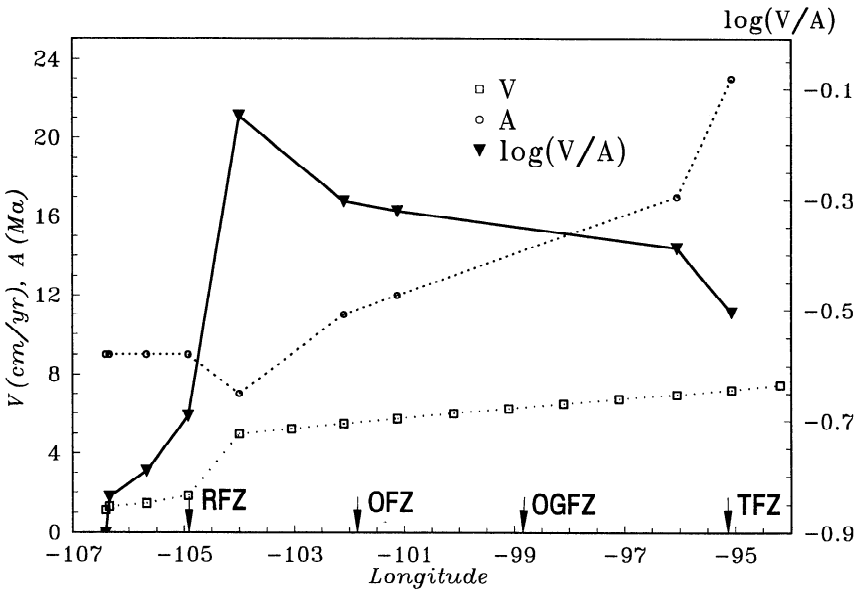

Fig. 2. Variation of age of subducting Rivera and Cocos plates [from *Klitgord and Mammerickx,* 1982], convergence velocity [from *DeMets et al.,* 1990] and parameter of coupling (log V/A) [*Kostoglodov,* 1988] along the Middle America trench (MAT). Arrows show the intruding points of main fracture zones at the MAT.

these create rather wide areas of interface contact (up to 100 km) between the fracture zones and the overthrusting continental plate.

We note a link between the fracture zones (RFZ, OFZ, OGFZ) and broad river valleys (Armería, Balsas and Rio Grande) which subdivide the costal mountain ridge (Sierra Madre del Sur) into sections corresponding to the segmentation of the underthrusting oceanic plate (Figure 1). The sites, where the fracture zones intrude into the MAT, are closely associated with underwater canyons on the continental slope. The northward orientated canyons probably exhibit traces of the migration of the intruding points in the east-southeast direction between early Miocene (9 m.y.) and late Miocene (6.5 m.y) which can be seen from the model of *Klitgord and Mammerickx* [1982]. The observed correlation between the location of those valleys and the fracture zones presumably reflects a relation between a degree of plate coupling and inelastic long-term deformation of the overthrusting continental lithosphere.

The variations of V, A and $\log(V/A)$ along the MAT are presented in Figure 2. The value of $\log(V/A)$, according to the V model [*Kostoglodov,* 1988], yields insight on the strength of coupling and the maximum magnitude of thrust earthquakes at a particular subduction zone. According to $\log(V/A)$ the strongest coupling and events with the largest magnitude should be expected at the Michoacan region (between RFZ and OFZ), where an M_s = 8.1 earthquake took place September 19, 1985 [*UNAM Seismology Group,* 1986; *Singh et al.,* 1988]. That was probably the largest possible earthquake that could occur in this zone, because the event ruptured practically all the area of the segment. In other segments farther south the coupling is lower. The maximum magnitude events encountered here were; for the Guerrero region (between OFZ and OGFZ), M_s = 7.9 [*Singh et al.,* 1981], M_s = 8.1 [*Anderson et al.,* 1989] of April 7, 1845 and M_s = 7.9 of January 24, 1899; for the Oaxaca region (between OGFZ and TR), M_s = 7.9 of May 11, 1870, M_s = 7.8 of June 17, 1928, August 23, 1965, and November 29, 1978.

The magnitude M_s = 8.2 of June 3, 1932, in Jalisco (RIV segment) is in contradiction with the V model since the estimated strength of coupling is too low (Figure 2). The resolution of this problem is that either the value of convergence velocity of the RIV plate is underestimated [*Carbotte and Macdonald,* 1992] or the relative velocity of the RIV and a hypothetic Jalisco block (JAL) of the NOAM [*Bandy et al.,* 1988] is higher than the convergence velocity of the RIV. The first is feasible in the sense that the Pacific-Rivera spreading rate is increasing with time (at least for the last 0.7 m.y.) [*DeMets and Stein,* 1990]. The second is less plausible because, assuming the mode and strength of coupling for the RIV is of the same type and order as for other segments of the COCOS, a value of $\approx$ 4 cm/yr for the relative velocity RIV-JAL would be expected. These extension rates for the Colima and Tepic-Chapala rifts are too high compared with geological estimates (slower than 0.1 cm/yr) [*Allan,* 1986].

DATA

For the background seismicity study the ISC catalog for the period from January 1963 to August 1987 has been merged with the USGS catalog for September 1987 to December 1990. All events with 4.5 $\leq m_b < 6.0$ were used (Figure 3). The hypocentral accuracy does not permit distinct separation of earthquakes into interplate and intraplate sets (Figure 4). Therefore the events within a band extending 150 km inland from the trench axis were presumably assigned to the interface zone and with the distance more than 150 km as occurring deeper inside the subducting plate. The space-time distribution of these two groups of events is shown in Figure 5.

The data set of historical thrust earthquakes in Mexico (Table 1) is based mostly on the recent catalog by *Anderson et al.* [1989]. They extensively revised earlier locations of epicenters and values of magnitudes given by *Singh et al.* [1981], *Abe* [1981], *González-Ruiz and McNally* [1988], *Nishenko and Singh* [1987 a, b, c], *Singh et al.* [1988], *Nuñez-Cornú and Ponce* [1989] using instrumental recordings of this century up to 1962 from Uppsala, Sweden, and introduced a new seismic moment - magnitude scale for the region:

$$\log M_o = 1.177\ M_s + 18.426. \qquad (1)$$

Epicenters of some earthquakes in the southeastern part of the MAT were corrected by a shift to the northeast of up to 100 km. The data for several earthquakes in that catalog still remain doubtful. The previous magnitude M_s = 7.9 of April 7, 1845 [*Singh et al.,* 1981],

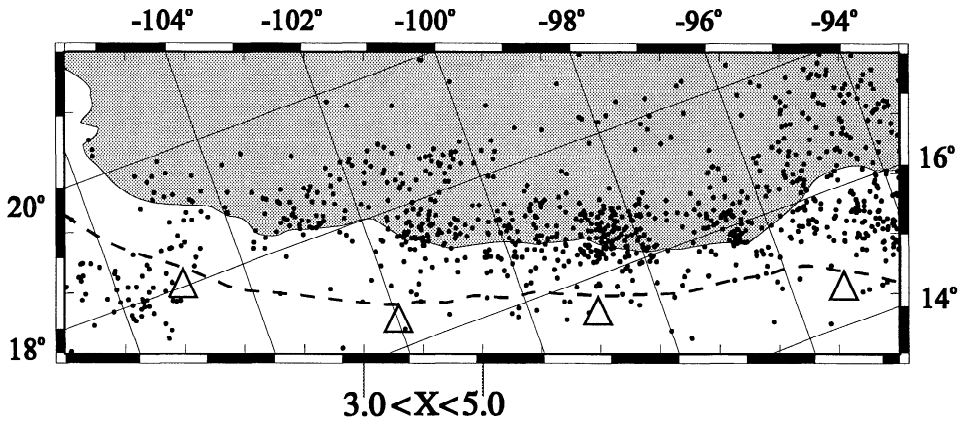

Fig. 3. Epicenters of events from ISC-USGS catalogs for 1963-1990, $4.5 \le m_b < 6.0$. The dashed line is the trench axis. The land area is shaded. The two vertical lines below indicate the position of cross section presented in Figure 4. Arrows show the intruding points of fracture zones at the MAT. The horizontal scale inside the frame is distance along the trench in 100 km.

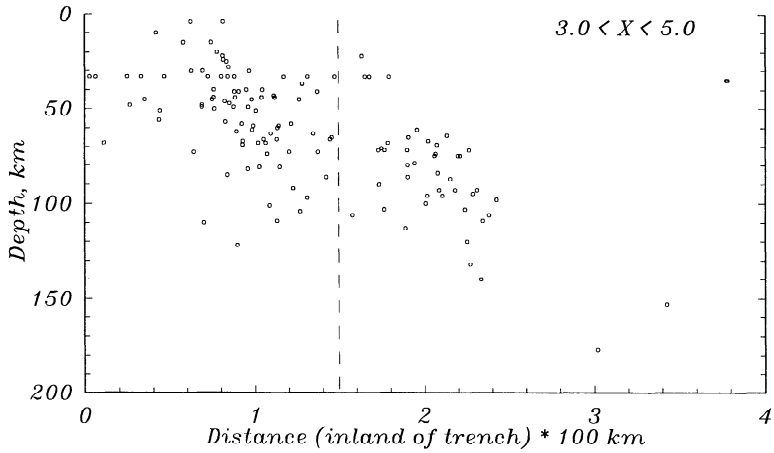

Fig. 4. Hypocenters of events from the ISC-USGS catalogs for 1963-1990, $4.5 \le m_b < 6.0$ for the cross section $3.0 < X < 5.0$ (see Figure 3). Dashed line indicates subdivision of earthquakes into interplate (< 150 km inland from the trench) and intraplate (> 150 km) sets.

was replaced with $M_s = 8.1$ which seems to be an overestimate. The epicenter of March 26, 1908, $M_s = 7.6 - 7.8$ [*Gutenberg and Richter*, 1954; *Nishenko and Singh*, 1987b] event was moved from 18°N, 99°W to 16.7°N, 99.2°W and exactly coincides with the April 15, 1907, $M_s = 7.7$, thrust earthquake [*Anderson et al.*, 1989] (see Figure 6b). It is improbable that the two events of that magnitude would occur within one year at the same location. An earthquake doublet occurred on January 6, 1948 (not included in Table 1) was classified by *Anderson et al.* [1989] as normal events ($M_s = 6.9$ and 7.0, depth = 80 km), while *González-Ruiz and McNally* [1988] have appraised it as double thrust event (combined $M_s \approx 6.7$, depth = 18 km).

We added to the catalog a number of events with $M_s \ge 6.0$ (Table 1) and used (1) to calculate seismic moments for the events which have no estimates of M_o. The locations and rupture areas are approximated by ellipses for the earthquakes of this data set and are shown in Figure 6 for three time periods 1800-1900, 1900-1950, and 1950-1990. Figure 6a clearly indicates a gap between 101°W and 102°W with a lack of information on historical events for the last century. The Guerrero seismic gap (100°W-101°W) is evident in Figure 6c.

In spite of these discrepancies and the obvious incompleteness of the catalog, it can nevertheless be used to obtain first approximation estimates of cumulative seismic moment and energy. Although the reliability of the catalog should be taken into account when using these estimates.

BACKGROUND SEISMICITY

The background seismicity was calculated as the total number of events and as the cumulative seismic moment within 50-km bands normal to the trench strike. A line connecting the two points 17.9°N, 105°W and 14.6°N, 96°W approximates the trench strike. The seismicity distribution along the MAT was evaluated for both the interplate and intraplate events. A general trend of increasing seismicity from the northwest to the southeast is evident on the space-number of events (S-N) and space-M_o (S-M_o) plots (Figures 7 and 8). A pronounced correlation was discovered between local peaks of interplate seismicity and locations of intruding points of the fracture zones (except perhaps the RFZ, where we do not have enough events for statistics). Other peaks may be attributed to the subduction of less evident bathymetric features, for example, the 97°W-fracture zone ("???" in Figure 1). A simple examination of the data (see, for example, Figure 5) confirms that aftershock activity has no significant bias to these peaks. For most of the fracture zones the higher levels of deep, intraplate seismicity can be observed on the S-M_o plot (Figure 8).

If we presume a general relation, that stronger plate coupling results in lower background seismicity, then it follows that the subduction of fracture zones is associated with lower coupling and presumably, a weaker interface. If so, relatively smaller magnitudes of large earthquakes [*Kelleher et al.*, 1973; *Kelleher and McCann*, 1976]

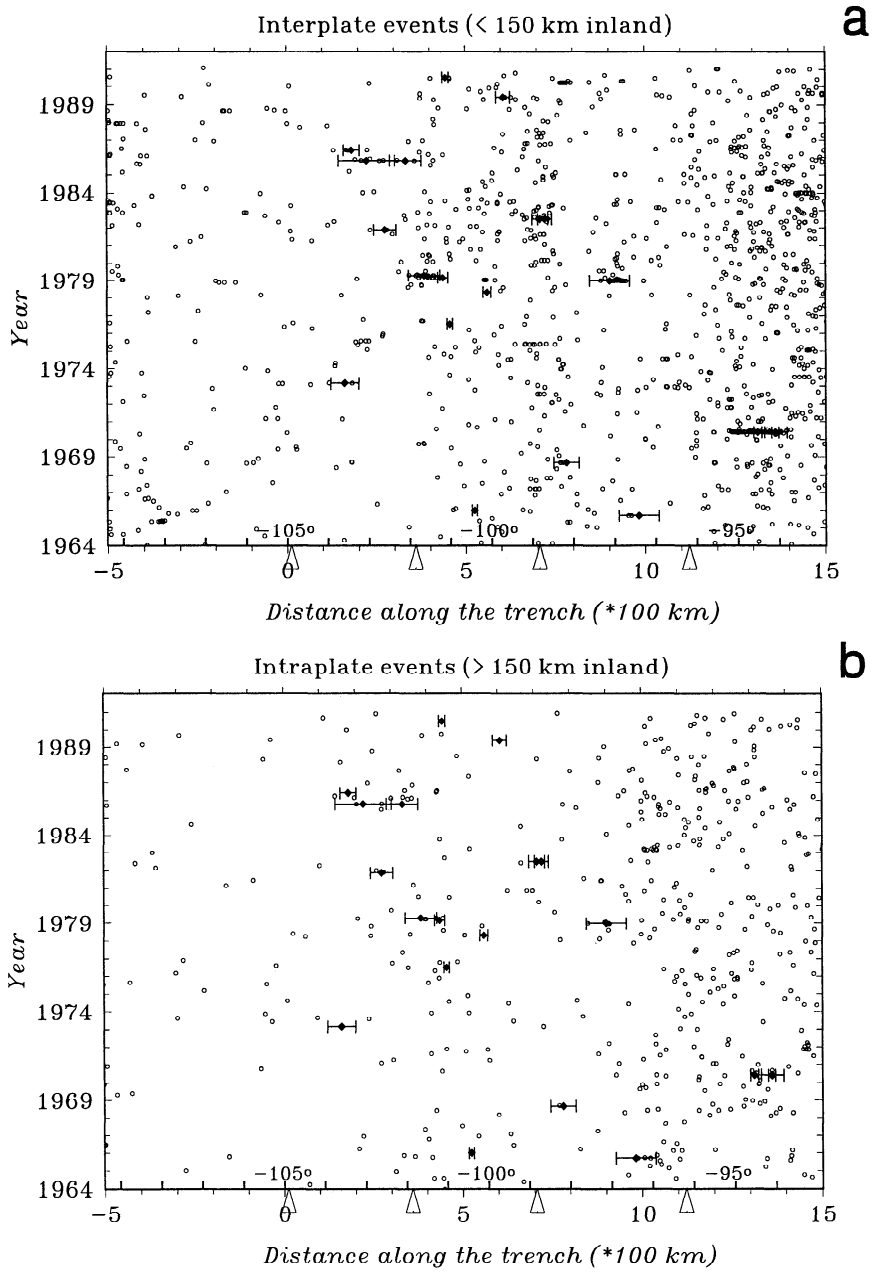

Fig. 5. Space-time plots of background seismicity (open circles) and rupture zones of great earthquakes (horizontal bars) (a) for the interplate events (< 150 km inland from the trench) and (b) for the intraplate events (> 150 km). Arrows show the intruding points of main fracture zones at the MAT.

and lower total seismic moment release should be expected at these zones.

CUMULATIVE SEISMIC MOMENT AND SEISMIC SLIP

The distribution of total cumulative seismic moment along the MAT was computed using the catalog of historic earthquakes with the routine formulated by V. Kostoglodov (submitted manuscript, 1991). To arrange this the region of the subduction zone between the two points 17.9°N, 105°W - 14.6°N, 96°W is subdivided into 68 strips, each 15 km wide, normal to the line approximating the trench strike. The rupture zones of earthquakes, presented as ellipses with an aspect ratio of 2 (average value for interplate thrust earthquakes), are computed using the rupture area estimates (S) acquired from seismic moment values (derived from *Kanamori* [1977]) as

$$\log S = 2/3 \log M_o - 14.73, \quad (2)$$

where S is in km^2 and M_o is in 10^{27} dyn cm. The seismogenic interface between the subducting COCOS and NOAM is relatively narrow, ≈ 35-45 km [*Suárez et al.*, 1990]. A great earthquake with magnitude of the order 7.7 would rupture the total width of the interface. To prevent the width of the rupture zone from exceeding the extreme value, we restrict it to 50 km for the largest earthquakes and adjust the aspect ratio to satisfy the calculated rupture area. The density distribution of seismic moment is simulated as uniform over the total rupture area. The center of each ellipse is taken as the epicentral point. These assumptions, of course, are artificial, but admissible because for most of the events in the catalog, the rupture zone configuration and the density distribution of M_o, as well as the exact epicenters

TABLE 1. Catalog of Large Mexican Thrust Earthquakes

Date	Time, UT	Latitude, °N	Longitude, °E	Depth, km	M_s	M_s^*	M_o, 10^{27} dyn cm	M_o^*, 10^{27} dyn cm	Reference
March 25, 1806	1700	18.90	-103.80		7.5		1.79	1.79	1
May 31, 1818		19.10	-103.60		7.7		3.08	3.08	1
May 4, 1820	2400	17.20	-99.60		7.6		2.35	2.35	1
Nov. 23, 1837	2800	20.00	-105.00		7.7		3.08	3.08	1
March 9, 1845	1330	16.60	-97.00		7.5		1.79	1.79	1
April 7, 1845	1600	16.60	-99.20		8.1	(7.9)[6]	9.11	9.11	1
May 5, 1854	0915	16.30	-97.60		7.7		3.08	3.08	1
May 11, 1870	2330	15.80	-96.70		7.9		5.30	5.30	1
March 27, 1872	0752	15.70	-96.60		7.4		1.37	1.37	1
March 16, 1874	0345	17.70	-99.10		7.3		1.04	1.04	1
Feb. 11, 1875		21.00	-103.80		7.5		1.79	1.79	1
March 9, 1875		19.40	-104.60		7.4		1.37	1.37	1
May 29, 1887		17.20	-99.80		7.2		0.80	0.80	1
Sept. 6, 1889		17.00	-99.70		7.0		0.46	0.46	1
Dec. 2, 1890		16.70	-98.60	30	7.2		0.80	0.80	1
Nov. 2, 1894	1835	16.50	-98.00		7.4		1.37	1.37	1
June 5, 1897	1222	16.30	-95.40		7.4		1.37	1.37	1
Jan. 24, 1899	2343	17.10	-100.50		7.9		5.30	5.30	1
Jan. 20, 1900	0633:30	20.00	-105.00		7.4		1.37	1.37	1
May 16, 1900	2012	20.00	-105.00		6.9		0.35	0.35	1
Sept. 23, 1902	2018	16.00	-93.00		8.3	(7.8)[5]	16.08	15.67	3
April 15, 1907	0608:06	16.70	-99.20		7.7		8.43	3.08	1
March 26, 1908	2303:30	16.70	-99.20	80	7.6		1.98	2.35	1
March 27, 1908	0345:30	17.00	-101.00		7.0		0.74	0.46	1
July 30, 1909	1051:54	16.80	-99.90		7.3		2.48	1.04	1
July 31, 1909	1843:10	16.60	-99.50		6.9		0.35	0.35	1
July 6, 1911	1102:42	17.50	-102.50	50	7.7		2.83	3.08	1
Dec. 16, 1911	1914:18	16.90	-100.50	50	7.6		2.35	2.35	1
Dec. 9, 1912	0832:24	15.50	-93.00		6.9			0.35	4
Nov. 21, 1916	0625:24	18.00	-100.00		6.8		0.27	0.27	1
Dec. 29, 1917	2250:20	15.00	-97.00		6.9		0.85	0.35	1
Nov. 16, 1925	1154:54	18.00	-107.00		7.0			0.46	4
March 22, 1928	0417:03	16.20	-95.50		7.5		1.79	1.79	1
June 17, 1928	0319:28	16.30	-96.70		7.8		3.90	4.04	1
Aug. 4, 1928	1828:17	16.80	-97.60		7.4		1.37	1.37	1
Oct. 9, 1928	0301:08	16.30	-97.30		7.6		2.35	2.35	1
June 3, 1932	1036:52	19.80	-104.00	20	8.2		9.10	11.95	1
June 18, 1932	1012:10	19.50	-103.50		7.8		7.30	4.04	1
Nov. 30, 1934	0205:16	19.00	-105.50		7.0		0.45	0.46	1
Dec. 14, 1935	2205:17	14.75	-92.50		7.4			1.37	4
Dec. 23, 1937	1311:58	17.10	-98.10		7.5		1.63	1.79	1
April 15, 1941	1909:51	18.80	-102.90		7.7		2.94	3.08	1
Aug. 6, 1942	2336:59	14.00	-91.00	50	7.9		5.55	5.30	4
Feb. 22, 1943	0920:45	17.60	-101.10		7.5		1.56	1.79	1
June 28, 1944	0758:54	15.00	-92.50		7.1		0.66	0.61	4
Sept. 29, 1950	0632:20	19.00	-107.00	60	6.6			0.16	4
Oct. 23, 1950	1613:20	14.50	-91.50		7.2			0.80	4
Dec. 14, 1950	1415:50	17.20	-98.10	16	7.1		0.89	0.61	1
Dec. 17, 1950	0108:02	16.65	-98.77		6.3		0.08	0.07	7
Dec. 26, 1950	1351:40	16.44	-98.56		6.5		0.13	0.12	7
Dec. 28, 1951	0920:25	17.00	-99.00	60	6.6		0.18	0.16	4
Nov. 17, 1953	1329:53	13.75	-92.00	40	7.1			0.61	4
July 28, 1957	0840:10	17.10	-99.10	18	7.5		5.13	1.79	1
May 11, 1962	1411:57	17.20	-99.60		7.2		0.90	0.80	1
May 19, 1962	1458:10	17.10	-99.60		6.9		0.80	0.35	1
Aug. 23, 1965	1946:02	16.30	-95.80	16	7.8		1.70	4.04	1
Dec. 9, 1965	0607:49	17.30	-100.00	57	6.0		0.04	0.03	2
Aug. 2, 1968	1406:44	16.60	-97.70	16	7.4		1.00	1.37	1
April 29, 1970	1122:36	14.47	-92.72	45	6.3		0.08	0.07	9
April 29, 1970	1401:34	14.45	-92.71	44	7.3		0.99	1.04	9
April 30, 1970	0832:58	14.58	-93.16	16	6.4		0.07	0.09	9

TABLE 1. (continued)

Date	Time, UT	Latitude, °N	Longitude, °E	Depth, km	M_s	M_s^*	M_o, 10^{27} dyn cm	M_o^*, 10^{27} dyn cm	Reference
Jan. 30, 1973	2101:18	18.40	-103.20	32	7.5		3.00	1.79	1
June 7, 1976	1426:39	17.40	-100.64	45	6.1		0.05	0.04	2
March 19, 1978	0139:14	17.03	-99.74	36	6.4		0.09	0.09	1
Nov. 29, 1978	1052:47	15.80	-96.80	18	7.8		3.20	4.04	1
Jan. 26, 1979		17.53	-100.79		6.6		0.18	0.16	8
March 14, 1979	1107:11	17.30	-101.40	20	7.6		2.70	2.35	1
Oct. 25, 1981	0322:13	17.80	-102.30	20	7.3		1.30	1.04	1
June 7, 1982	0652:34	16.30	-98.40	15	6.9		0.27	0.35	1
June 7, 1982	1059:40	16.40	-98.50	20	7.0		0.25	0.46	1
Sept. 19, 1985	1317:49	18.10	-102.70	16	8.1		11.70	9.11	1
Sept. 21, 1985	0137:12	17.60	-101.80	20	7.6		3.12	2.35	1
April 30, 1986	0707:18	18.40	-103.00	20	7.0		0.30	0.46	1
April 25, 1989		16.58	-99.46		6.9		0.39	0.35	8
May 31, 1990		17.14	-100.86		6.2		0.06	0.05	8

M_s^*, Other estimates. M_o^*, Seismic moment from the relation (1). Reference are (1) *Anderson et al.* [1989], (2) *Singh et al.* [1984], (3) *Nuñez-Cornú and Ponce* [1989], (4) *Abe* [1981], (5) *Nishenko and Singh* [1987b], (6) *Singh et al.* [1981], (7) *González-Ruiz and McNally* [1988], (8) Ponce et al. (unpublished manuscript, 1990) and (9) *Yamamoto and Mitchell* [1988].

are unknown. For the recent earthquakes with good estimates of the rupture area and hypocenter an appropriate correction can be done.

The seismic moment released by each earthquake (j) on strip (i) can be estimated as

$$M_{o_{ij}} = \int_{S_{ij}} \rho_j(x)\, dS, \tag{3}$$

where S_{ij} is the area of strip (i) covered by the rupture ellipse of the event (j), $\rho_j(x)$ is a density distribution of M_o in the event (j), x is a coordinate along the trench strike. Then the cumulative moment release M_{o_i} can be obtained by summation for all events. Finally, a seismic moment release rate ($\dot{M}_o$) is evaluated for each strip from time-M_o distributions (Figure 9).

Figure 10 presents the distributions of M_o and $\dot{M}_o$ versus distance along the MAT. As was hypothesized from the analysis of background seismicity, the lowest values of cumulative seismic moment indeed correspond to the areas of the fracture zone impingement at the MAT, thereby supporting the suggestion of low coupling. Nevertheless, an average NW-SE trend expected from the V model is absent probably because of some overestimates of magnitudes and poor loci for the historical events above mentioned.

The seismic moment release rate plot (Figure 10) produced three sharp outlying peaks which are a consequence of lack of sufficient data (Figure 9c). In fact, $\dot{M}_o$ should not vary so abruptly on a short distance. Therefore these peaks are deleted by linear interpolation. The refined curve correlates prevalently with the M_o plot. In the zone from 94°W to 100°W the correlation is better because the catalog is more complete. A slight trend of $\dot{M}_o$ apparently reflects an overall change of coupling.

A similar procedure may be applied to estimate cumulative seismic energy release (W_i) along the trench. The Gutenberg-Richter relation combined with the relation between energy and rupture area (derived from *Kanamori* [1977])

$$\log W = 1.5\, M_s + 11.8$$

$$W \approx cS^{2/3},$$

where $c \approx 0.625 \times 10^{18}$ erg/km^2, gives in this case

$$\log S \approx M_s - 4.0. \tag{4}$$

Equation (4) overestimates the rupture area in comparison to equation (2). To keep the rupture length close to the observed one we fix in this case the aspect ratio of 2 in spite of the fact that the rupture width becomes greater than the maximum possible for the largest events. Both the W_i and $\dot{W}_i$ distributions (Figure 11) exhibit the average northwest-southeast trend which agree with the tendency of lowering coupling. The cumulative seismic energy released from 1963 to 1990 ($W63_i$ in Figure 11) reveals no significant correlation with the background seismicity (see Figures 7 and 8).

A three-dimensional (3-D) plot of cumulative seismic energy versus time and distance is shown in Figure 12. The influence of the fracture zones (OFZ and OGFZ) as well as the incompleteness of the catalog for the strips with numbers from 10 to 34 can be easily seen.

The average seismic slip rate ($\dot{U}$) was evaluated for each strip (i) from the estimates of $\dot{M}_o$ by

$$\dot{U}_i = \frac{\dot{M}_i}{\mu\, l_i\, D}, \tag{5}$$

where the shear modulus μ is taken as 4×10^{11} dyn cm^{-2} [*Anderson et al.*, 1989], length of the strip $l_i = 15$ km, and width of the interface rupture zone $D = 50$ km.

The values of $\dot{U}$ are systematically lower then those for convergence velocities given by the NUVEL 1 plate motion model [*DeMets et al.*, 1990] (Figure 13) except in the RIV segment. There V is likely to be underestimated.

An appraisal of average errors involved in our estimates of $\dot{U}$ can be made using the uncertainties in the determination of M_o. For 36 events in Table 1 the values of M_o and M_o^* were obtained by different techniques (27 events are from *Anderson et al.* [1989]). The deviation of those values varies from 1.1% up to 137.8% with a mean of 29.3%. Consequently, the error in the estimates of $\dot{U}$ may be at least of the same order.

The seismic slip is defined by the ratio $\gamma = \dot{U}/V$. It varies along the MAT in accordance with the structure of the subducting COCOS plate. The maxima of seismic slip occur at the central parts of the main segments of oceanic lithosphere that are separated by the fracture zones. The theoretical estimates of γ obtained from (A6), in general fit the observed data when the constant a is fixed as $a = 1$ and $b = 0.18 \pm 0.04$ (10^{-6}cm yr^{-2}) (Figure 14). Large variations in $\dot{U}$ along the trench, in addition to errors, do not permit us to reliably resolve

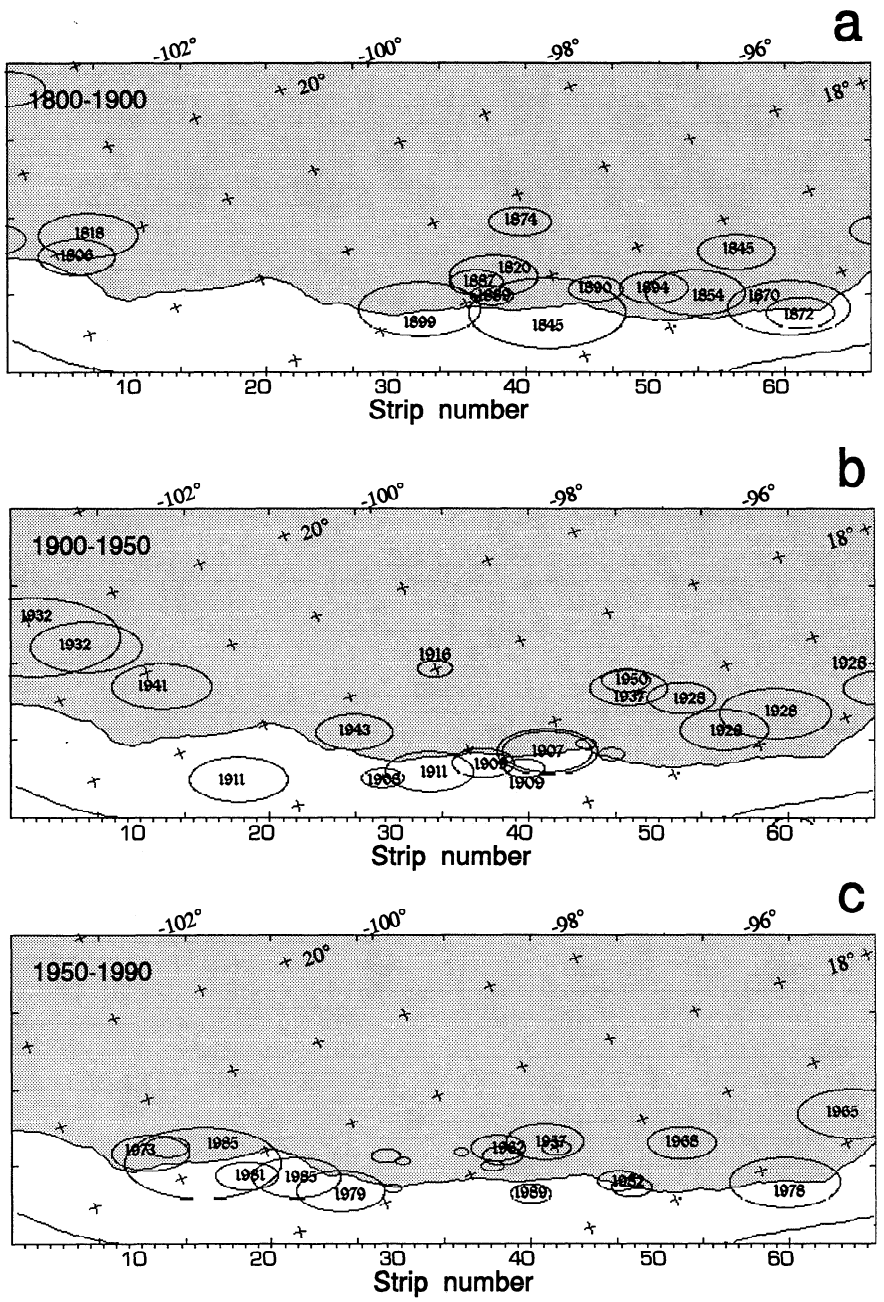

Fig. 6. Location and rupture areas approximated by ellipses for earthquakes from the catalog of large Mexican thrust events (Table 1) for the three time intervals: (a) 1800-1900, (b) 1900-1950, (c) 1950-1990. The lower horizontal scale is a strip number. Each strip is of 15 km width. Numbers inside the ellipses are years.

deviations of a from $a = 1$. The estimate of a also strongly depends on the accepted value of μ (5). In our case we choose the value of $\mu = 4 \times 10^{11}$ dyn cm^{-2} to normalize the estimates of $\dot{U}$ so that the maximum of $\dot{U}$ would not exceed the convergence velocity of the COCOS (Figure 13).

Migration of Strong Events

A time-space plot for the historical earthquakes (Figure 15) shows some indications of probable northwestward migration of large earthquakes with an average rate of $\approx$ 10 km/yr. Two 60- to 80-yr sequences of seismicity migration separated by a 40- to 50-yr interval may be traced. A southward migration of seismicity of the same order rate ($\approx$ 7 km/yr) has been distinguished by S. Barrientos (submitted manuscript, 1991) in central Chile for large earthquakes of this century. *Elsasser* [1969] type models of stress diffusion in a coupled lithosphere/asthenosphere plate system are usually applied to interpret this migration [*Bott and Dean,* 1973; *Anderson,* 1975; *Li and Kisslinger,* 1984]. The deformation front propagates in this system with a low velocity. It is specified by a ratio of shear modulus of the lithosphere to viscosity of the asthenosphere and depends slightly on local inhomogeneities of the lithosphere such as fracture zones.

According to the model, such a front propagating along the subduction plate boundary may trigger large thrust earthquakes in an adjacent segment of finite length if it has already accumulated a sufficient amount of elastic strain energy. It is seen in Figure 15 that the last deformation front passed the Guerrero seismic gap (between 100°W and 101°W) in 1965-1975 not inducing any big event. Therefore either that hypothetical front does not provoke

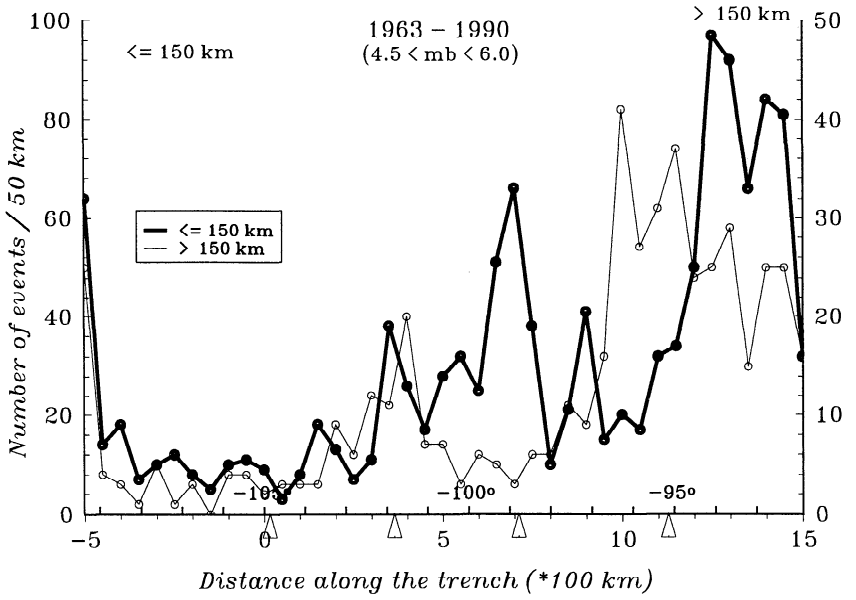

Fig. 7. Distribution of the background seismicity along the MAT (space-number of events). General trend of increasing seismicity from the northwest to the southeast corresponds to a reduction of plate coupling. A correlation between the local peaks of seismicity and intruding points of the main fracture zones (arrows) indicates relatively low level of plate coupling at these areas. Interplate events are < 150 km inland from the trench, and intraplate events > 150 km.

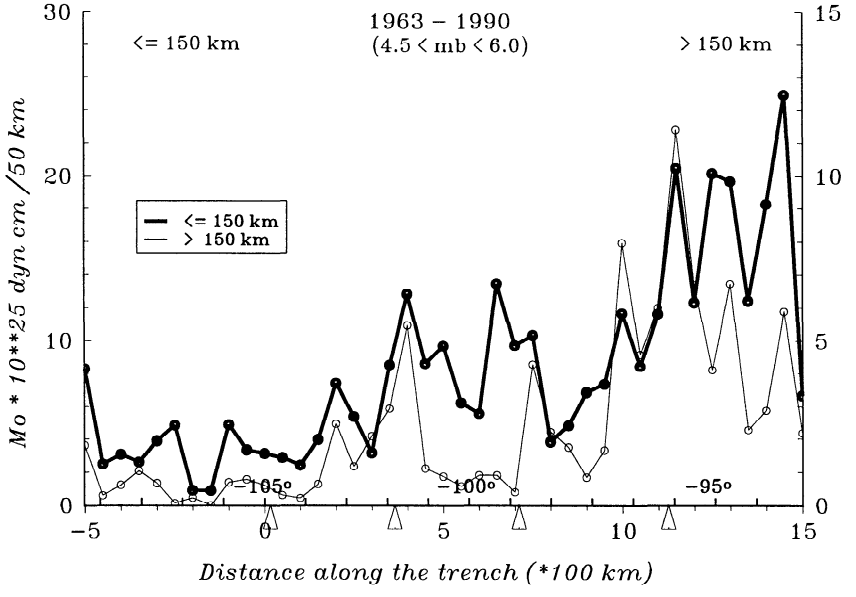

Fig. 8. Distribution of the background seismicity along the MAT (space-M_o). Interplate events are < 150 km inland from the trench, and intraplate events > 150 km.

earthquakes or the Guerrero gap apparently has a relatively low rate of elastic strain energy accumulation because of the weaker plate coupling in this region.

DISCUSSION

Detailed studies of subduction seismicity at the MAT show that a general correlation exists between the degree of mechanical plate coupling and the seismicity regime. The stronger coupling causes larger magnitude earthquakes, higher seismic moment release rate, and higher seismic slip. These relations are in good agreement with physical models of plate interaction at the interface zone (for example, the V model). The observed inverse correlation with background seismicity is more difficult to interpret. One of the plausible, but qualitative explanations may be an increase of yield stress in the highly coupled and more homogeneous interface which prevents nucleation and rupture of small asperities [*Lay et al.*, 1982].

A characteristic of subduction and seismicity at the MAT is that significant segmentation occurs and is associated with the convergence of fracture zones. Relatively high background seismicity together with a deficiency of cumulative seismic moment and seismic moment release rate provide evidence for low coupling at these areas.

There is still no acceptable model for the subduction mechanism of bathymetric features such as fracture zones [*Kelleher and McCann*, 1976; *Burbach et al.*, 1984; *LeFevre and McNally*, 1985; *McCann and Habermann*, 1989]. The topographic features associated with fracture zones are apparently supported by the elastic flexure of the lithosphere [*Kogan and Kostoglodov*, 1981], therefore an entire

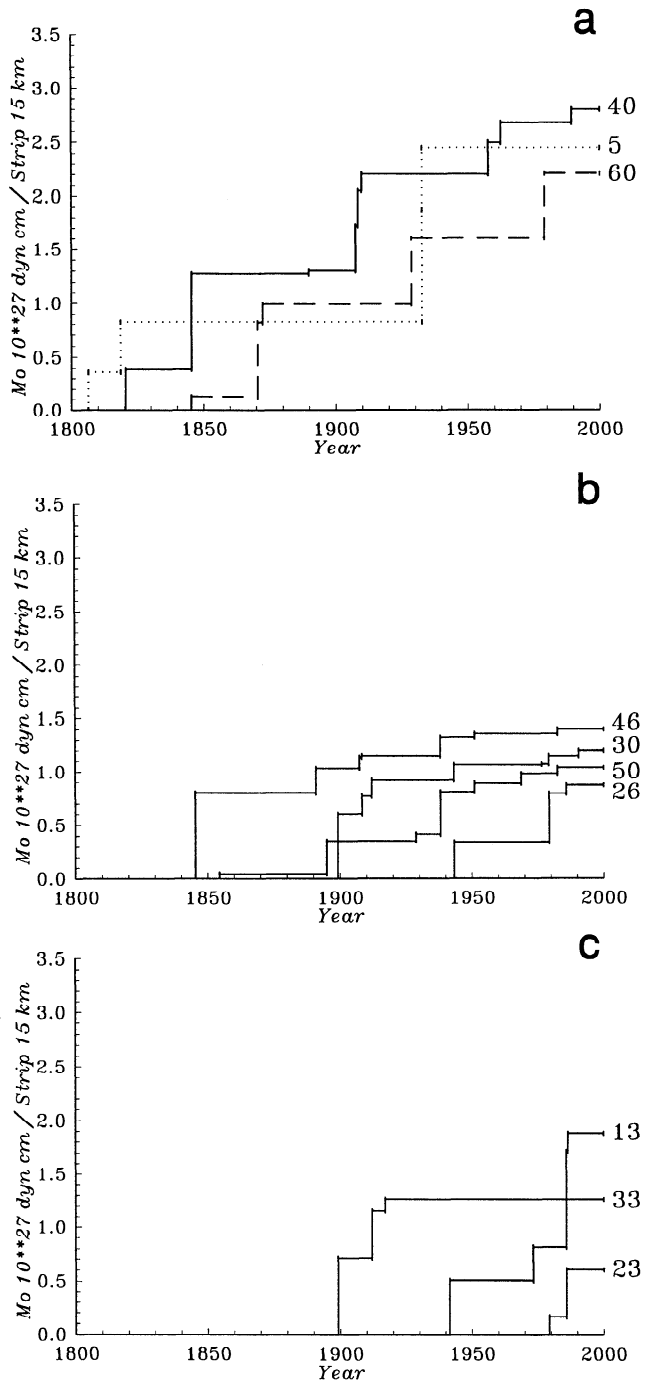

Fig. 9. Time-seismic moment distributions for the strips of 15 km width, which are perpendicular to the strike of the trench (see Figure 6), from different areas. (a) Zones of high coupling, (b) areas of low coupling close to the intruding points of fracture zones and (c) zones with a lack of historical data. Numbers placed near the curves indicate the strip numbers.

structure of fracture zone at least may not be more buoyant than compared to the surrounding seafloor. The supposition of negatively buoyant fracture zones relative to ordinary oceanic lithosphere may be the most feasible [*Detrick and Purdy,* 1980]. The buoyancy of the lithosphere is probably the principal factor controlling subduction which can be investigated with numerical modeling. The other approach to the problem is a detailed study of the stress regime with data obtained from local seismic networks located in the regions of fracture zone subduction.

An important characteristic of the seismicity regime is the seismic moment release rate. For the MAT its estimates are better for the southeast part where the historical catalog is more complete and the higher correlation between $\dot{M}_o$ and the cumulative moment can be seen (Figure 10). In the region of the O'Gorman fracture zone subduction, $\dot{M}_o$ drops 2-3 times which is an indication of the low degree of plate coupling. Unfortunately, a lack of historical data for the region of the Orozco fracture zone and the Guerrero seismic gap does not allow us to come to a firm conclusion regarding the lower coupling. Indirectly, for the OFZ it comes from the analysis of background seismicity and an assumption that a convergence mechanism for the OGFZ and OFZ is similar. The Guerrero gap is located on a transition from the OFZ to the zone of high coupling and probably has a coupling of moderate degree.

Although some indication of seismicity migration may be recognized on the space-time plot of large events (Figure 15), and the estimate of velocity of this migration corresponds to the model of stress diffusion, there is not sufficient evidence that this mechanism is a trigger for large earthquakes. Moreover, the migration pattern may be just a result of successive alternation of large earthquakes along the particular subduction zone.

Seismic slip obtained from $\dot{M}_o$ and approximated with equation (A6) for the Mexican subduction zones does not provide the possibility to ascertain the value of a, and hence to distinguish between the seismic (elastic) and aseismic (plastic or nonrecoverable) components of the strain. The distribution of seismic slip along the MAT shows large variation because of the influence of the fracture zones. The distribution of tectonic strain buildup along the MAT is hard to retrieve from the seismological data alone, and will have to wait until an adequate model of fracture zone subduction exists. Major constrains on that can come from geological and geodetical studies of recent crustal deformation near sites of ridge-subduction.

CONCLUSIONS

The main conclusions that can be drawn from this study are summarized as follows:

1. Background seismicity ($4.5 \le m_b < 6.0$) and cumulative seismic moment estimated from a catalog of large historical earthquakes can be used to study the coupling strength in subduction zones of continental type such as the Middle American convergence system. A concurrent increase of background seismicity and reduction of cumulative seismic moment together with seismic release rate is an indication of a drop in plate coupling. For the Middle America trench the last two effects are in good agreement with a prediction of the V model of the subduction interface [*Kostoglodov,* 1988].

2. Convergence of the main fracture zones of the COCOS plate under the NOAM plate creates rather broad areas with apparently low coupling and low seismic release rates. While a physical mechanism of this phenomenon is still obscure, some insight into the problem can be gained by study of irregularities in structural and geological properties of oceanic fracture zones, through local seismological study of the stress regime and by numerical modeling.

3. Normalized seismic slip rates along the MAT estimated from seismic moment release rates are systematically lower than convergence velocities of the COCOS plate given by the NUVEL 1 plate motion model. The seismic slip estimates contain noticeable errors and large variations along the MAT caused by subduction of the fracture zones. Nevertheless the average seismic slip deduced from the V model is a good approximation to observed values. Unfortunately, from average seismic slip it is impossible to infer any limitation on tectonic strain buildup.

4. Assuming a validity of the V model, the strongest earthquake of this century, $M_s = 8.2$ June 3, 1932, in Jalisco (Rivera plate zone),

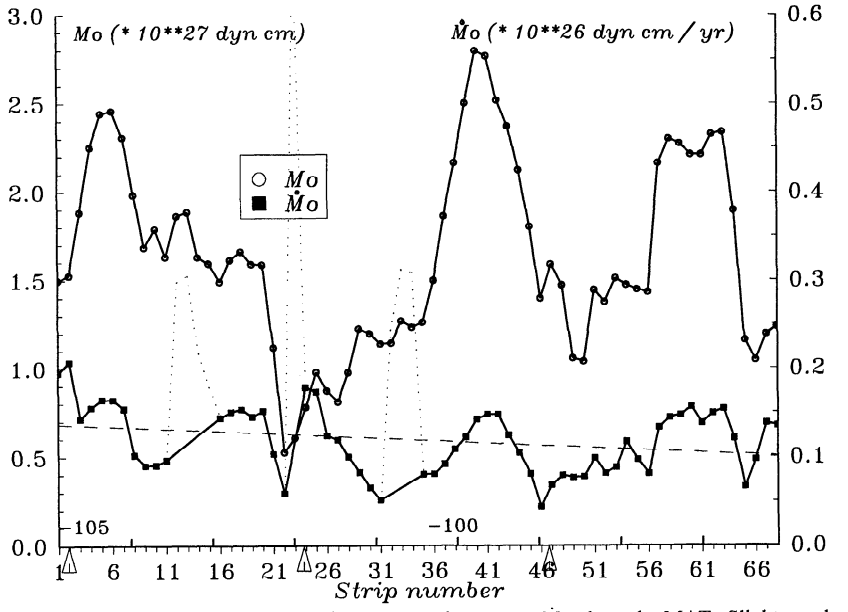

Fig. 10. Cumulative seismic moment, M_o, and seismic moment release rate, $\dot{M}_o$, along the MAT. Slight trend of $\dot{M}_o$ is indicated in the northwest-southeast direction corresponding to decreased plate coupling. Locations of main fracture zones coincide with the areas of relatively low values of M_o and $\dot{M}_o$. Intruding points of fracture zones are shown by arrows. The dotted line indicates outlying peaks of $\dot{M}_o$ which are a consequence of lack of sufficient data. The dashed line is the trend of $\dot{M}_o$.

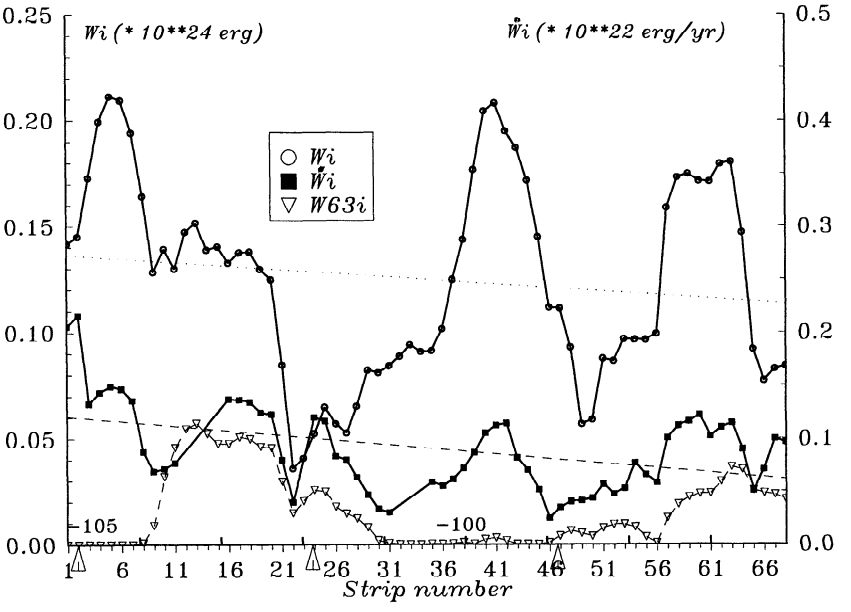

Fig. 11. Cumulative seismic energy, W, and seismic energy release rate, $\dot{W}$, distribution. Slight trends are indicated in the northwest-southeast direction. Locations of main fracture zones coincide with the areas of relatively low values of W and $\dot{W}$ which supports the hypothesis of weak coupling at those zones. $W63_i$ - cumulative seismic energy released from 1963 to 1990. The dotted line is the trend of W, and the dashed one is the trend of $\dot{W}$.

requires a minimum value of convergence velocity of ≈ 4 cm/yr. This is in contradiction with the NUVEL 1 and other plate motion models but conforms qualitatively to a probable acceleration of the Pacific-Rivera spreading during the last 0.7 Ma.

5. Probable northwest migration of strong earthquakes with a velocity of ≈ 10 km/yr along the MAT may be perceived on the space-time plot of the historical events. Although models exist which can explain a migration of this kind by the triggering effect of a deformation front, there remains insufficient evidence in support of such models.

APPENDIX: THE VISCOUS INTERFACE MODEL (V MODEL)

In the paper of *Kostoglodov* [1988], a model that included extensive sediment subduction and viscous interaction of lithospheric plates at convergent zones was applied to derive simple relations between seismic and global tectonic parameters. Here we give only the most important assumptions and main results of this V model which are used in the present study.

Figure A1 illustrates a simplified scheme of subduction involving consolidated, high viscosity pelagic sediments. If the strength of

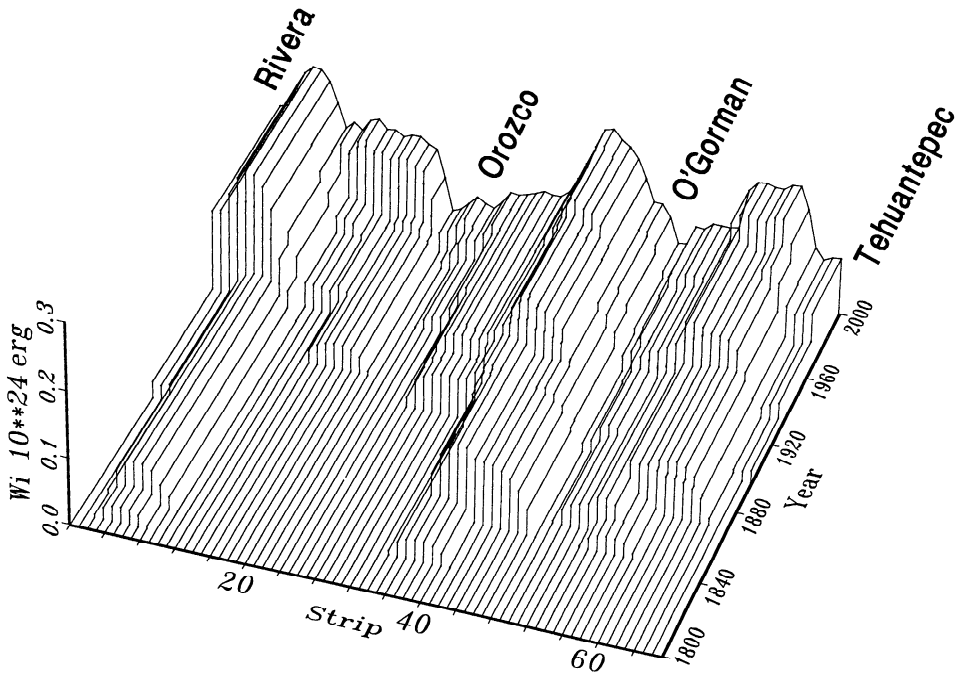

Fig. 12. A 3-D plot of cumulative seismic energy versus time and distance along the MAT. The influence of the fracture zones as well as the incompleteness of the historical catalog for the strips from 10 to 34 can be seen.

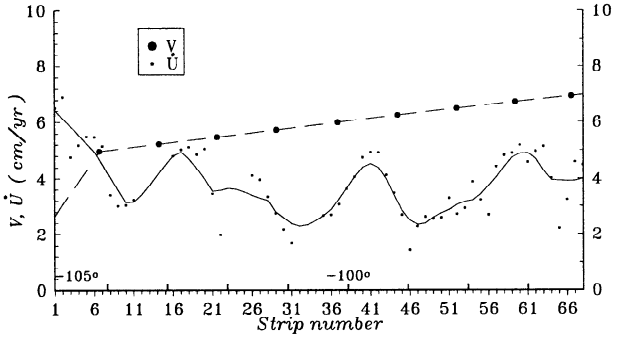

Fig. 13. Distribution of seismic slip rate, $\dot{U}$, along the MAT. The normalized values of $\dot{U}$ for the Cocos plate are systematically lower than those for the convergence velocity, V, from NUVEL 1 plate motion model [*DeMets et al.*, 1990].

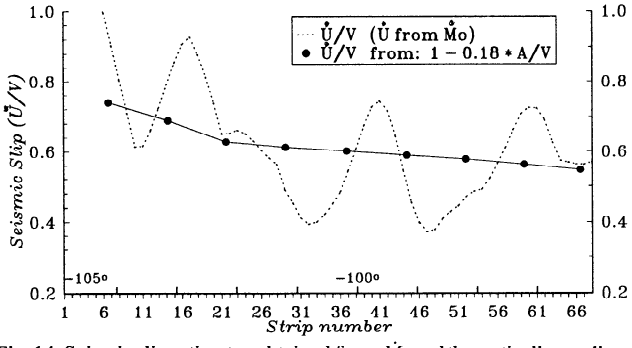

Fig. 14. Seismic slip estimates obtained from $\dot{M}_o$ and theoretically predicted from the V model.

mechanical coupling at the interface zone is defined as the maximum shear stress, τ_m, at the base of the overthrusting plate, then

$$\tau_m = \frac{\eta(V-V')}{h} \approx \frac{\eta V}{h}, \quad V' << V. \tag{A1}$$

Here h is thickness and η is viscosity of the interface layer. V is convergence velocity and V' is velocity at the lower surface of the overriding plate. $V' << V$, when the leading edge of upper plate reaches the maximum deformation before the largest rebound event.

Assuming that older oceanic lithosphere subducts a relatively larger amount of pelagic sediments or that the thickness of the interface layer, h, depends on the age, A, of subducting plate, as

$$h = \alpha v A , \tag{A2}$$

where α is a constant, and v is an average pelagic sedimentation rate, then the strength of coupling is

$$\tau_m = C_2 V/A , \quad C_2 = \eta/\alpha v. \tag{A3}$$

If the maximum elastic strain energy accumulated by the leading edge of the continental plate in a particular subduction zone is totally released seismically in the greatest possible earthquake, the relation between maximum magnitude, M_w, and the parameter of coupling, $\log(V/A)$, can be obtained by

$$M_w = 4\log(V/A) + 2\log C + \text{const}, \tag{A4}$$

$$C \approx \frac{L^2}{3EH} C_2^2,$$

where L and H are the length and height of that part of the continental plate which suffers the main deformation (see Figure A1). E is Young's modulus of the continental lithosphere.

The expression (A4) is derived presuming an elastic strain energy balance for interseismic and coseismic periods. Although (4), in general, satisfies currently available data, the value of the coefficient in front of $\log(V/A)$ estimated from the data is slightly lower than 4. This signifies that only some part of total strain energy being accumulated by the subduction system is released seismically.

If the velocity changes linearly within the viscous interface layer, the average velocity, $\bar{V}'$, of the overthrusting edge during the interseismic period is

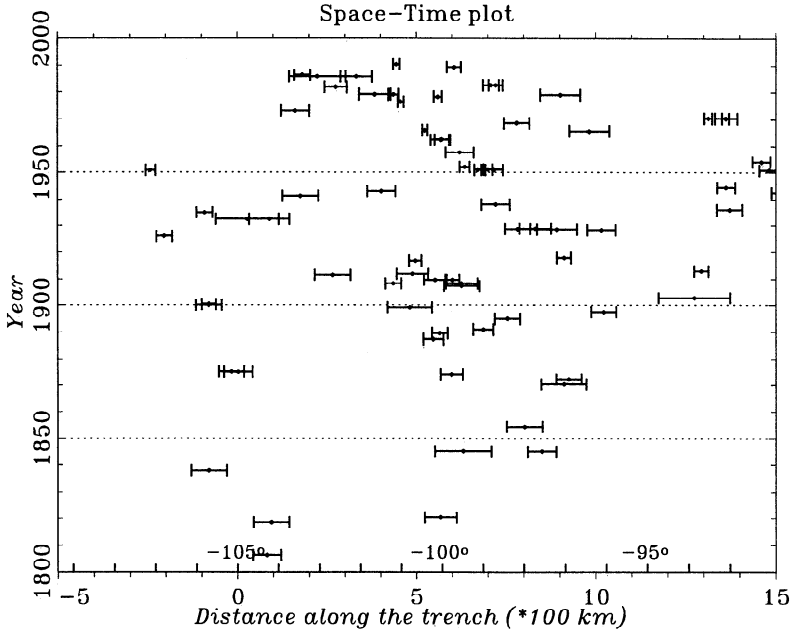

Fig. 15. Space-time plot for historical earthquakes. Horizontal bars are proportional to the rupture length of the earthquakes. Some indications of NW migration of large earthquakes with an average rate of 10 km/yr may be noticed. During the last cycle of propagation of the hypothetical deformation front a strong event in the area of the Guerrero seismic gap (100°W-101°W) was not induced. The Guerrero gap apparently has a relatively low rate of elastic strain energy accumulation because of its weaker coupling.

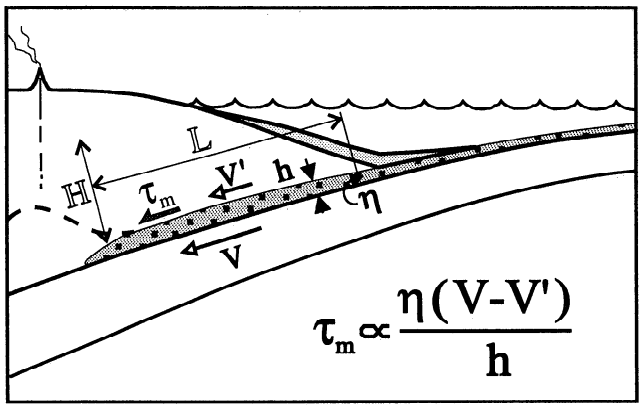

Fig. A1. The simplified scheme illustrating the V model. The strength of mechanical coupling, i.e., the maximum shear stress on the lower surface of overriding plate, τ_m depends on the thickness h and viscosity η of sediments which are drawn into the interface zone, and on the relative velocity between plates $(V - V')$. The thickness of the interface sedimentary layer could be up to 1-1.5 km in some subduction zones if the viscosity is of the order of 10^{19} P [*Sorokhtin and Lobkovsky*, 1976]. Terrigenous sediments filling the trench are shown by light shading. Dark shaded, dotted layer depicts subducted, consolidated sediments.

$$\bar{V}' \approx V - bA, \qquad \text{(A5)}$$

where b is a constant. Then assuming that the seismic slip rate, $\dot{U} = a\bar{V}'$, $a = const.$, the seismic slip (relative seismic slip velocity, $\gamma = \dot{U}/V$) can be defined as:

$$\gamma \approx a - b(A/V). \qquad \text{(A6)}$$

Here $a = 1$ if $\dot{U} \approx V'$, and $a < 1$ if $\dot{U} < V'$, i.e., when some deformation of the upper plate is partially released in aseismic slip or transformed into inelastic deformation. The estimates of $\dot{U}$ usually contain considerable errors which make it practically impossible to determine a deviation of a from $a = 1$.

Acknowledgments. We would like to thank Shri Krishna Singh, Dan Byrne, Cinna Lomnitz and Ramon Zúñiga for useful discussions. Dan Byrne suggested many important improvements to the manuscript. Numerous corrections and valuable critical reviews which were made by two anonymous referees, Albert Tarantola and Senior Editor William J. Hinze were also appreciated and helped us to refine the paper noticeably. This work was supported by Consejo Nacional de Ciencia y Tecnología, México.

REFERENCES

Abe, K., Magnitudes of large shallow earthquakes from 1904 to 1980, *Phys. Earth Planet. Inter., 27,* 72-92, 1981.

Allan, J.F., Geology of the northern Colima and Zacoalco grabens, southwest Mexico: Late Cenozoic rifting in the Mexican volcanic belt, *Geol. Soc. Am. Bull., 97,* 473-485, 1986.

Anderson, D., Accelerated plate tectonics, *Science, 187,* 1077-1079, 1975.

Anderson, J.G., S.K. Singh, J.M. Espindola, and J. Yamamoto, Seismic strain release in the Mexican subduction thrust, *Phys. Earth Planet. Inter., 58,* 307-322, 1989.

Bandy, W., T.W.C. Hilde, and J. Bourgois, Redefinition of the plate boundaries between the Pacific, Rivera, Cocos and North American plates at the north end of the Middle America trench (abstract), *Eos Trans. AGU, 69,* 1415, 1988.

Bott, M.H.P., and D.S. Dean, Stress diffusion from plate boundaries, *Nature, 243,* 339-341, 1973.

Burbach, G.V., C. Frohlich, W.D. Pennington, and T. Matumoto, Seismicity and tectonics of the subducted Cocos plate, *J. Geophys. Res., 89,* 7719-7735, 1984.

Carbotte, S., and K. Macdonald, East Pacific Rise 8°-10°30'N: Evolution of ridge segments and discontinuities from SeaMARC II and three-dimensional magnetic studies, *J. Geophys. Res., 97,* 6959-6982, 1992.

Chael, E., and G.S. Stewart, Recent large earthquakes along the Middle American trench and their implications for the subduction process, *J. Geophys. Res., 87,* 329-338, 1982.

Couch, R., and S. Woodcock, Gravity and structure of the continental margins of southwestern Mexico and northwestern Guatemala, *J. Geophys. Res., 86,* 1829-1840, 1981.

DeMets, C., and S. Stein, Present-day kinematics of the Rivera plate and implications for tectonics in Southwestern Mexico, *J. Geophys. Res., 95,* 21,931-21,948, 1990.

DeMets, C., R.G. Gordon, D.F.Argus, and S.Stein, Current plate motions, *Geophys. J. Int., 101,* 425-478, 1990.

Detrick, R., and G. Purdy, The crustal structure of the Kane fracture zone from seismic refraction studies, *J. Geophys. Res., 85,* 3759-3777, 1980.

Dewey, J.W., and G. Suárez, Seismotectonics of Middle America, in *Neotectonics of North America, Decade Map,* edited by D.B. Slemmons et al., vol. 1, chapt. 17, pp. 309-321, 1991.

Dirección General de Oceanografia Naval, *Carta Isobatimétrica, Zona Económica Exclusiva y Márgines Continentales del Oeste de México,* in Atlas/Memoria del Levantamiento Geofísico de la Zona Económica Exclusiva y Márgen Continental Oeste de México. Gravedad, Magnetismo y Batimetria, Secr. de Mar., Mansanillo, México, 1987.

Elsasser, W.M., Convection and stress propagation in the upper mantle, in *The application of modern physics to the Earth and planetary interiors,* edited by S.K. Runcorn, pp. 223-246, Wiley-Interscience, New York, 1969.

González-Ruiz, J.R., and K.C. McNally, Stress accumulation and release since 1882 in Ometepec, Guerrero, Mexico: Implications for failure mechanisms and risk assessment of a seismic gap, *J. Geophys. Res., 93,* 6297-6317, 1988.

Gutenberg, B., and C.F. Richter, *Seismicity of the Earth,* 2nd ed., pp. 161-234, Princeton University Press, Princeton, N. J., 1954.

Kanamori, H., The energy release in great earthquakes, *J. Geophys. Res., 82,* 2981-2987, 1977.

Kelleher, J., and W. McCann, Buoyant zones, great earthquakes, and unstable boundaries of subduction, *J. Geophys. Res., 81,* 4885-4896, 1976.

Kelleher, J., L. Sykes, and J. Oliver, Possible criteria for predicting earthquake locations and their application to major plate boundaries of the Pacific and Caribbean. *J. Geophys. Res. 78,* 2547-2585, 1973.

Klitgord, K., and J. Mammerickx, East Pacific rise: Magnetic anomaly and bathymetric framework, *J. Geophys. Res., 87,* 6725-6750, 1982.

Kogan, M.G., and V.V. Kostoglodov, Isostasy of fracture zones in the Atlantic Ocean, *J. Geophys. Res., 86,* 9248-9258, 1981.

Kostoglodov, V.V., Sediment subduction: A probable key for seismicity and tectonics at active plate boundaries, *Geophys. J., 94,* 65-72, 1988.

Lay, T., H. Kanamori, and L. Ruff, The asperity model and the nature of large subduction zone earthquakes, *Earthquake Predict. Res., 1,* 3-71, 1982.

LeFevre, L.V., and K.C. McNally, Stress distribution and subduction of aseismic ridges in the Middle America subduction zone, *J. Geophys. Res., 90,* 4495-4510, 1985.

Li, V.C., and C. Kisslinger, Stress transfer and nonlinear stress accumulation at subduction-type plate boundaries - Application to the Aleutians, *Pure Appl. Geophys., 122,* 812-830, 1984.

Mammerickx, J., and K. Klitgord, Northern East Pacific rise: evolution from 25 m.y.b.p. to the present, *J. Geophys. Res., 87,* 6751-6759, 1982.

McCann, W.R., and R.E. Habermann, Morphologic and geologic effects of the subduction of bathymetric highs, *Pure Appl. Geophys., 129,* 41-69, 1989.

McNally, K.C., and J.B. Minster, Nonuniform seismic slip rate along Middle America trench, *J. Geophys. Res., 86,* 4949-4959, 1981.

Molnar, P., and L.R. Sykes, Tectonics of the Caribbean and Middle American regions from focal mechanisms and seismicity, *Geol. Soc. Am. Bull., 80,* 1639-1684, 1969.

Nishenko, S.P., and S.K. Singh, Relocation of the great Mexican earthquake of 14 January 1903, *Bull. Seismol. Soc. Am., 77,* 256-259, 1987a.

Nishenko, S.P., and S.K. Singh, Conditional probabilities for recurrence of large and great interplate earthquakes along the Mexican subduction zone, *Bull. Seismol. Soc. Am., 77,* 2095-2114, 1987b.

Nishenko, S.P., and S.K.Singh, The Acapulco-Ometepec, Mexico, earthquakes of 1907-1982: evidence of variable recurrence history, *Bull. Seismol. Soc. Am., 77,* 1359-1367, 1987c.

Nuñez-Cornú, F., and L. Ponce, Zonas sísmicas de Oaxaca, México: Sismos máximos y tiempos de recurrencia para el período 1542-1988, *Geofis. Int., 28,* 587-641, 1989.

Ruff, L., and H. Kanamori, Seismicity and subduction process, *Phys. Earth Planet. Inter., 23,* 240-252, 1980.

Ruff, L., and H. Kanamori, Seismic coupling and uncoupling at subduction zones, *Tectonophysics., 99,* 99-117, 1983.

Singh, S.K., and F. Mortera, Source time functions of large Mexican subduction earthquakes, morphology of the Benioff zone, age of plate, and their tectonic implications, *J. Geophys. Res., 96,* 21,487-21,502, 1991.

Singh, S.K., L. Astiz, and J. Havskov, Seismic gaps and recurrence periods of large earthquakes along the Mexican subduction zone: A reexamination, *Bull. Seismol. Soc. Am., 71,* 827-843, 1981.

Singh, S.K., M. Rodriguez, and J.M. Espindola, A catalog of shallow earthquakes of Mexico from 1900 to 1981, *Bull. Seismol. Soc. Am., 74,* 267-279, 1984.

Singh, S.K., E. Mena, and R. Castro, Some aspects of source characteristics of 19 September 1985 Michoacan earthquake and ground motion amplification in and near Mexico city from strong motion data, *Bull. Seismol. Soc. Am., 78,* 451-477, 1988.

Sorokhtin, O.G., and L.I. Lobkovsky, The mechanism of subduction of oceanic sediments into a zone of underthrusting of lithospheric plates, *Izv. Acad. Sci. USSR, Phys. Solid Earth, Engl. Transl., 12,* 289-293, 1976.

Suárez, G., T. Monfret, G. Wittlinger, and C. David, Geometry of subduction and depth of the seismogenic zone in the Guerrero gap, Mexico, *Nature, 345,* 336-338, 1990.

UNAM Seismology Group, The September 1985 Michoacan earthquakes: Aftershock distribution and history of rupture, *Geophys. Res. Lett., 13,* 573-576, 1986.

Yamamoto, J., and B.J. Mitchell, Rupture mechanics of complex earthquakes in southern Mexico, *Tectonophysics., 154,* 25-40, 1988.

V. Kostoglodov and L. Ponce, Instituto de Geofisica, UNAM, 04510 México D.F., México.

(Received September 1, 1992;
revised June 2, 1993;
accepted June 8, 1993.)